Chemical Engineering Journal 165 (2010) 365–369

Contents lists available at ScienceDirect

Chemical Engineering Journal

journal homepage: www.elsevier.com/locate/cej

Hydrothermal synthesis of monoclinic WO_3 nanoplates and nanorods used as an electrocatalyst for hydrogen evolution reactions from water

Dong Jin Ham [a], Anukorn Phuruangrat [a,b,*], Somchai Thongtem [b], Jae Sung Lee [a,**]

[a] Eco-friendly Catalysis and Energy Laboratory (NRL), Department of Chemical Engineering, School of Environmental Science and Engineering, Pohang University of Science and Technology, San 31, Hyoja-dong, Pohang 790-784, Republic of Korea
[b] Department of Physics and Materials Science, Faculty of Science, Chiang Mai University, Chiang Mai 50200, Thailand

ARTICLE INFO

Article history:
Received 21 May 2010
Received in revised form 31 August 2010
Accepted 3 September 2010

Keywords:
Monoclinic WO_3
Nanorods
Nanoplates
Hydrothermal reaction
Hydrogen evolution reaction

ABSTRACT

Monoclinic WO_3 (m-WO_3) nanoplates and nanorods were successfully synthesized by a simple hydrothermal process using sodium tungstate dihydrate ($Na_2WO_4{\cdot}2H_2O$), ammonium nitrate (NH_4NO_3) and polyethylene glycol (PEG) as initial precursors. Phase, morphologies and electrochemical properties of the products were characterized by X-ray diffraction (XRD), scanning and transmission electron microscopy (SEM, TEM), high-resolution transmission electron microscopy (HRTEM), cyclic voltammetry (CV) and linear sweep voltammetry (LSV). The effect of NH_4NO_3 concentration on the formation of the pure phase of m-WO_3 nanomaterial was studied. The product synthesized under NH_4NO_3-free condition was pure orthorhombic $WO_3{\cdot}0.33H_2O$ (o-$WO_3{\cdot}0.33H_2O$) phase. By adding and increasing the amount of NH_4NO_3 to the solution, m-WO_3 phase started to form and became pure m-WO_3 phase when 1.50 g NH_4NO_3 was used. The morphology of m-WO_3 was nanoplates, and became nanorods by PEG adding. The nanostructured m-WO_3 showed much higher electrocatalytic activity for hydrogen evolution from water than that of the commercial bulk m-WO_3, including the m-WO_3 nanorods with slightly better than the m-WO_3 nanoplates.

1. Introduction

Shape-controlled synthesis of transition metal oxide nanomaterials with low dimensional morphologies, including zero dimensional (0D), one dimensional (1D) and two dimensional (2D) is highly significant, for both fundamental science and technical applications, because they have unique physical and chemical properties including optical, magnetic, luminescent and electronic. For example, 0D nanomaterials have potential applications in biological imaging and diagnostics, magnetic nanoprobes, information storage, chemical sensors, and highly active catalysts. 1D and 2D nanomaterials have important applications in lasers, display devices, nanoscale electronic circuits, and can be utilized as active sites for catalysts and applied in sensing nanodevices for electronic, magnetic, and optical applications [1–5].

Tungsten oxide (WO_3), an important *n*-type semiconductor, has received wide attention owing to its promising application for electrochromic and photochromic devices, secondary batteries, photocatalysts, gas sensors, heterogeneous catalysts, solar energy devices, field electron emission and electrocatalyst in electrolysis of water for hydrogen production [4–10]. The monoclinic WO_3 (m-WO_3) has been focused by scientists and researchers in last decades because it is more stable phase than any other WO_3 structures [1,2,5,7,11]. The m-WO_3 structure has a distorted ReO_3-type consisting of a three-dimensional network of WO_6 octahedrons [11]. The WO_3 with different morphologies such as nanorods [12], nanocubes [5], nanoplates [1,2] and nanoparticles [6,8] was successfully synthesized by various methods, including inorganic–organic hybrid method [1,2], hydrothermal reaction [5,12], thermal oxidization [8], pulsed spray pyrolysis deposition technique [10], and wet chemical precipitation [13]. Among them, hydrothermal process offers significant advantages in controlling over the product shape and size at low processing temperature, extreme homogeneity, and cost effectiveness [14,15] by combining with soft templates as chelating ligands and capping reagents such as polyethylene glycol (PEG) [16,17], polyvinyl alcohol (PVA) [18,19] and ethylene diamine tetra acetate (EDTA) [20,21] to produce 1D nanomaterials. In this work, PEG was selected to direct the 1D growth of self-assembled WO_3.

* Corresponding author at: Department of Physics and Materials Science, Faculty of Science, Chiang Mai University, Chiang Mai 50200, Thailand and Department of Chemical Engineering, School of Environmental Science and Engineering, Pohang University of Science and Technology, San 31, Hyoja-dong, Pohang 790-784, Republic of Korea.
** Corresponding author. Tel.: +82 54 279 2266; fax: +82 54 279 5528.
E-mail addresses: phuruangrat@hotmail.com (A. Phuruangrat), jlee@postech.ac.kr (J.S. Lee).

1385-8947/$ – see front matter © 2010 Elsevier B.V. All rights reserved.
doi:10.1016/j.cej.2010.09.003

The present research was focused on the synthesis of monoclinic WO_3 (m-WO_3) nanoplates and nanorods for use as electrocatalyst for hydrogen evolution reaction (HER) by simple hydrothermal method using sodium tungstate dihydrate ($Na_2WO_4{\cdot}2H_2O$) as tungsten source, ammonium nitrate (NH_4NO_3) for controlling monoclinic structure, and polyethylene glycol (PEG, MW = 20,000) for controlling 1D shape. The synthesis parameters, leading to different phases and morphologies of WO_3 nanomaterials, were studied and discussed in this report. The phase and morphologies of m-WO_3 nanomaterials were investigated by X-ray diffraction (XRD), scanning electron microscopy (SEM), and transmission electron microscopy (TEM). The electrocatalytic hydrogen evolution reaction from water for different morphologies of WO_3 (nanoplates and nanorods) was investigated by cyclic voltammogram (CV) and linear sweep voltammetry (LSV).

2. Experiment

2.1. Preparation of m-WO_3 nanoplates and nanorods

The precursor was prepared by dissolving 2.0 g sodium tungstate dihydrate ($Na_2WO_4{\cdot}2H_2O$) as tungsten source in 50 ml of 6 M HCl solution under 30 min stirring to form H_2WO_4 solution. Then 30 ml of 1.50 g ammonium nitrate (NH_4NO_3) solution for controlling monoclinic structure was mixed in the solution for the synthesis of WO_3 nanoplates. To prepare WO_3 nanorods, 1.0 g of polyethylene glycol (PEG, MW = 20,000) for controlling 1D shape was added to the mixture of $Na_2WO_4{\cdot}2H_2O$ and NH_4NO_3. The PEG-added solution was stirred until achieving the completely colorless solution. The precursors with and without PEG solution were transferred into 100 ml Teflon-lined stainless steel autoclave, which was processed at 200 °C for 24 h in an electric oven. At the completion of the process, the resulting precipitates of light-yellow (nanoplates) and yellow-green (nanorods) were separated by filtering, washed with distilled water to remove the remaining ions and ethanol to facilitate the evaporation of water, and finally dried at 100 °C in air for 12 h.

2.2. Characterization of phase and morphology

The phase of the products was characterized using X-ray diffraction (Mac Science M18XHF diffractometer) with a Ni-filter and Cu-K_α X-ray radiation source, and morphology using Hitachi, S-4200, scanning electron microscope (SEM) and JEOL, JEM-2100F, transmission electron microscope (TEM) and high resolution transmission electron microscope (HRTEM).

2.3. Electrochemical characterization

The glassy carbon electrode (geometric surface area of glassy carbon = 0.0707 cm^2), Pt wire, and Ag/AgCl electrode were used as working, counter and reference electrodes, respectively. 1 M H_2SO_4 solution was used as electrolyte for cyclic voltammogram and linear sweep voltammetry performed on a Princeton Applied Research (PAR) potentiostat. The working electrodes were prepared by catalytic ink – dispersing 20 mg catalyst in 1000 μl distilled water and 10 μl of 5 wt% Nafion under 30 min ultrasonic radiation. A known amount of catalytic ink was dropped on a glassy carbon electrode and dried at 100 °C for 4 min. Coat on the surface of the glassy carbon electrode by 10 μl of 5 wt% Nafion, and leave for evaporation.

3. Results and discussion

XRD patterns of WO_3 synthesized in the solutions with and without PEG by the hydrothermal process at 200 °C for 24 h are shown in Fig. 1. All diffraction peaks are consistent with those expected for monoclinic WO_3 phase (m-WO_3), comparing to the JCPDS No. 83-0950 as standard [22]. No any other impurities were detected, showing that the products are pure phase. Peak intensities are high and sharp, indicating that the products are very good crystalline. It is worth to note that the strong diffraction peak of the (0 0 2) plane is higher than those of other diffraction planes, revealing the m-WO_3 structure with highly anisotropic growth in the *c*-axis [7,11,23,24].

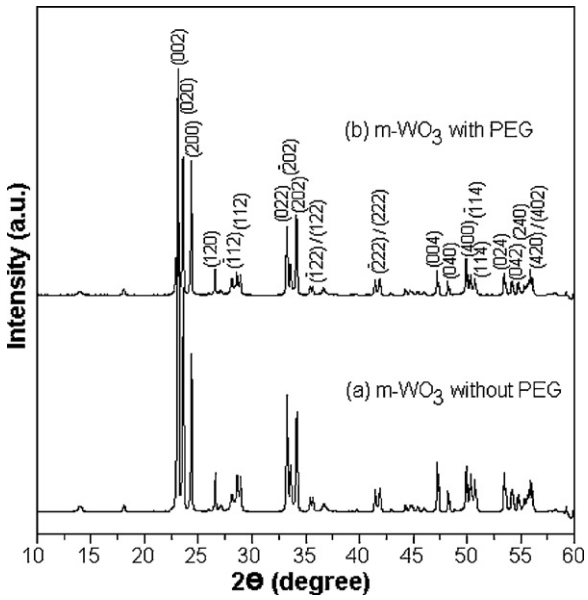

Fig. 1. XRD patterns of m-WO_3 synthesized by hydrothermal method at 200 °C for 24 h using $Na_2WO_4{\cdot}2H_2O$, NH_4NO_3 with and without PEG.

To investigate the role of NH_4NO_3 in determining the phase of the product, m-WO_3 nanostructures were synthesized by varying the amount of NH_4NO_3 and using different kinds of salts. Fig. 2 shows the XRD patterns of the products synthesized using different masses of NH_4NO_3 (0.00–1.50 g) at 200 °C for 24 h. In NH_4NO_3-free solution, XRD pattern shows the pure orthorhombic $WO_3{\cdot}0.33H_2O$ phase (o-$WO_3{\cdot}0.33H_2O$) corresponding to the JCPDS No. 35-0270 [22]. When NH_4NO_3 was added to the solution, and its masses were increased from 0.25 to 1.00 g, the products were mixtures of o-$WO_3{\cdot}0.33H_2O$ and m-WO_3 phases. The content of o-$WO_3{\cdot}0.33H_2O$ decreased with the increase in the NH_4NO_3 concentration. Pure m-WO_3 phase was achieved when 1.50 g NH_4NO_3 was added to the solution. Other inorganic salts of NH_4Cl, $LiNO_3$ and KNO_3 were used to investigate the formation of m-WO_3 phase. Their XRD patterns are shown in Fig. 3, and were interpreted as the mixtures of m-WO_3 and o-$WO_3{\cdot}0.33H_2O$ phases. These results indicate that NH_4NO_3 and its different concentrations play the role in controlling the pure phase of monoclinic WO_3 structure.

Morphologies of the products were investigated by scanning electron microscope (SEM) and transmission electron microscope (TEM). SEM image of m-WO_3 synthesized without PEG (Fig. 4) shows the nanoplates over the range of 0.50–1.00 μm wide and 0.10–0.20 μm thick. TEM and HRTEM images of m-WO_3 nanostructure synthesized in the PEG-added solution are shown in Fig. 5. The low and high magnifications clearly indicated as the m-WO_3 nanorods with 8–10 nm in diameter and 50–200 nm in length, but no detection of other morphologies. The HRTEM image (inset of Fig. 5b) shows lattice fringe of crystallographic planes that are perpendicular to the m-WO_3 nanorods with 3.76 Å space, corresponding with that of the (0 2 0) plane of the JCPDS No. 83-0950 as standard. This demonstrated that the m-WO_3 nanorods grew along the [0 1 0] direction, difference from the report of Bathe and Patil

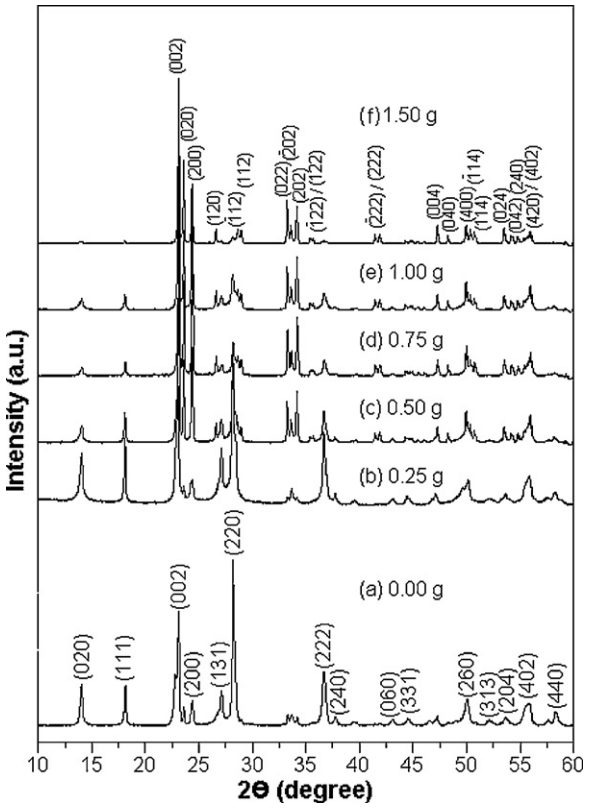

Fig. 2. XRD patterns of the products synthesized using different masses of NH_4NO_3.

– growing along the *c*-axis direction [7]. In conclusion, the morphologies of the as-synthesized m-WO_3 nanostructure changed from nanoplates to nanorods by PEG adding. Thus PEG played a role in controlling the m-WO_3 nanostructured morphologies.

Formation mechanisms of m-WO_3 nanoplates and nanorods are able to be described as follows [24,25].

$$2H^+ + WO_4^{2-} + nH_2O \leftrightarrow H_2WO_4{\cdot}nH_2O \quad (1)$$

$$H_2WO_4{\cdot}nH_2O \leftrightarrow WO_3 + (n+1)H_2O \quad (2)$$

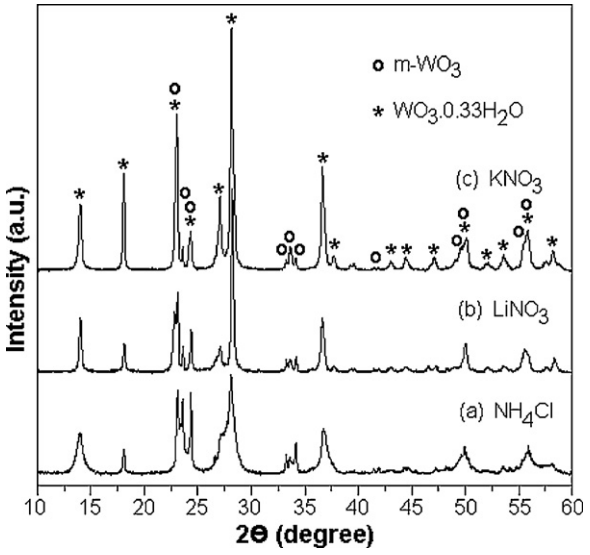

Fig. 3. XRD patterns of the products synthesized using 1.50 g of (a) NH_4Cl, (b) $LiNO_3$ and (c) KNO_3.

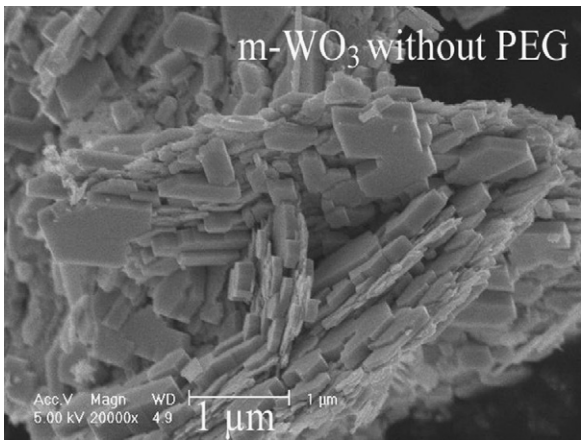

Fig. 4. SEM image of m-WO_3 synthesized in the PEG-free solution by hydrothermal method at 200 °C for 24 h.

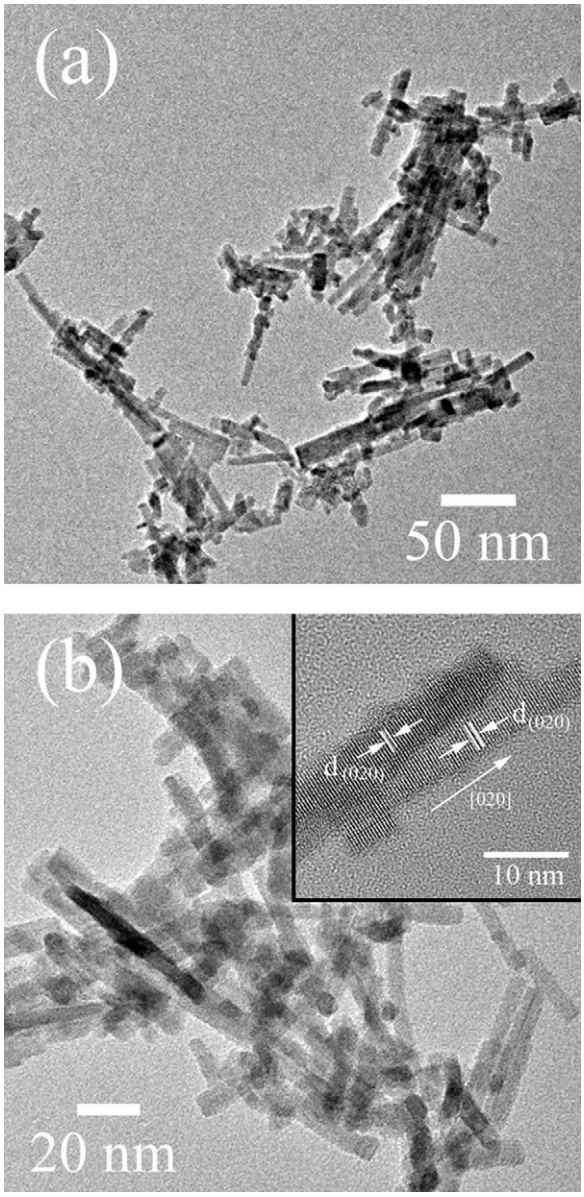

Fig. 5. TEM images of m-WO_3 nanorods at (a) low and (b) high magnifications, including its HRTEM image (inset).

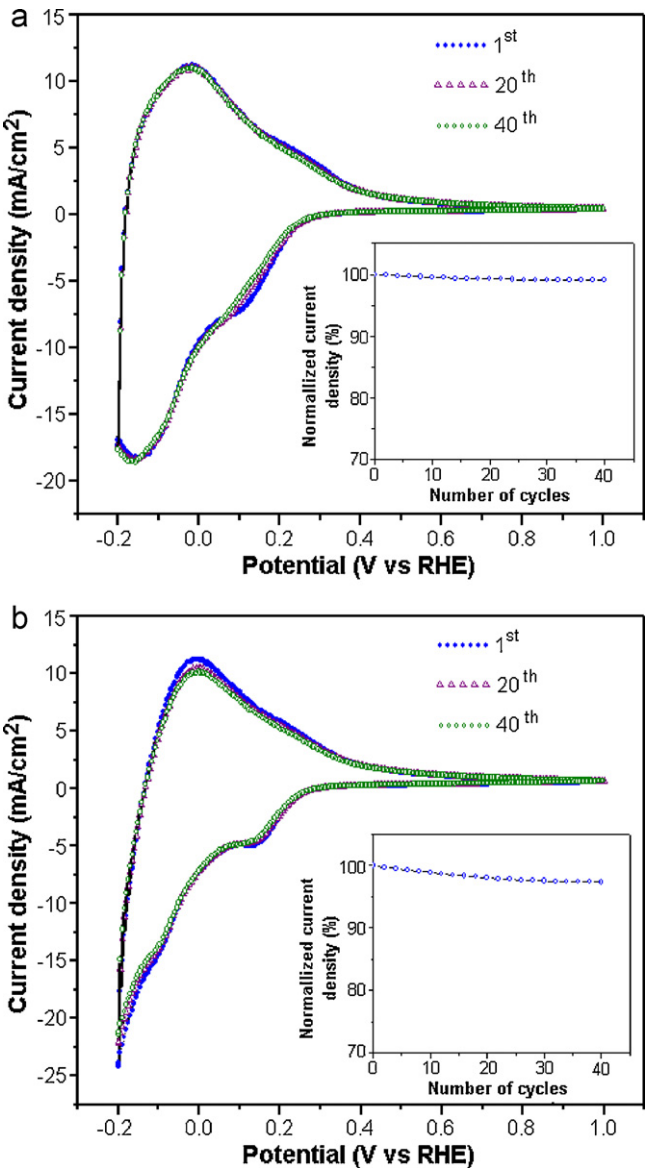

Fig. 6. Cyclic voltammograms and stability for 40 cycles (insets) of (a) m-WO_3 nanoplates and (b) m-WO_3 nanorods.

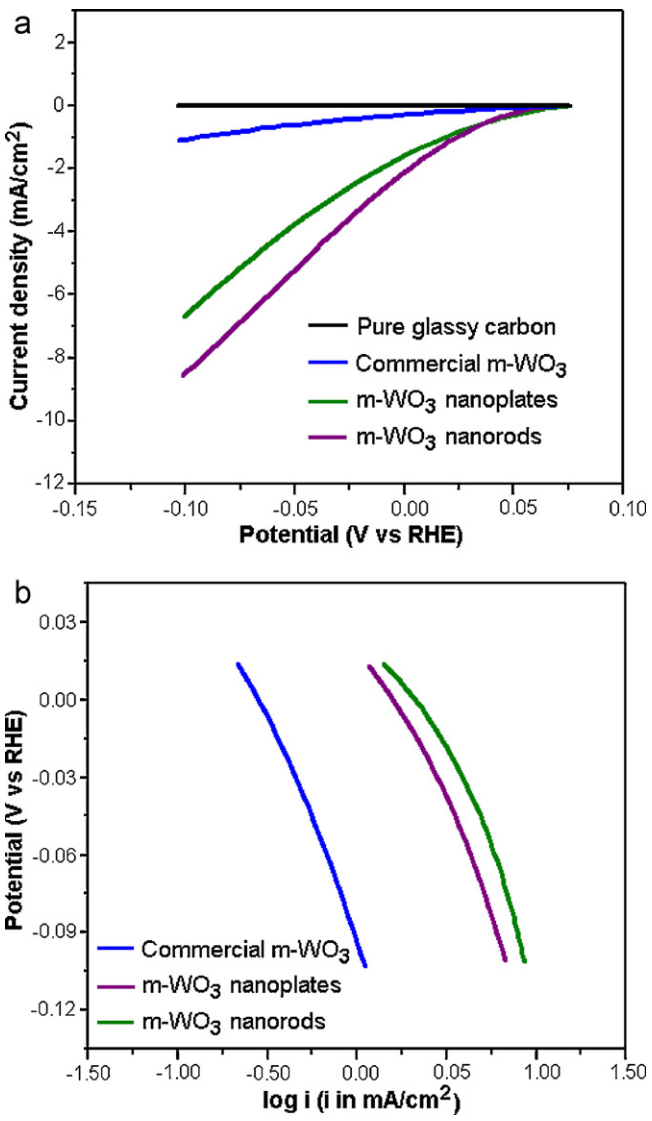

Fig. 7. (a) Linear voltammograms, and (b) Tafel plots of pure glassy carbon, commercial m-WO_3, m-WO_3 nanoplates and m-WO_3 nanorods.

By dissolving sodium tungstate dihydrate, the colorless solution formed. Then this colorless solution transformed into the yellow one upon adding of HCl solution, thus show the possible formation of tungstic acid solution [23,26]. Under hydrothermal treatment, the tungstic acid in the presence of NH_4NO_3 with and without PEG was dissolved and decomposed into different shapes of m-WO_3. For m-WO_3 in PEG-free solution under hydrothermal system, WO_3 nuclei rapidly formed from the precursor, subsequently these nuclei served as seeds, grew due to self-assembled process and developed into m-WO_3 nanoplates [2]. When PEG was added, the self-assembled process was inhibited by heavy capping of PEG at the very beginning of the nucleation, and small nuclei formed [27]. Initially, PEG adsorbed on the surface of m-WO_3 nuclei, which subsequently grew in the [0 1 0] direction via the self-diffusion process. Finally, m-WO_3 nanorods were synthesized and detected.

The hydrogen evolution reaction (HER) of m-WO_3 nanoplates and nanorods was studied using cyclic voltammetry (CV), and linear sweep voltammetry (LSV), including the Tafel plots in comparison with the commercial m-WO_3 – the particle size was below 50 nm and the surface area was around 16 m^2/g via peak calculation of XRD. The active capacity values of m-WO_3 nanoplates and nanorods were measured by CV in 1 M H_2SO_4 solution over the potential range of −0.20 to +1.00 V at a scan rate of 50 mV/s for 40 cycles. Fig. 6 shows the cyclic voltammograms of 2D m-WO_3 nanoplates and 1D m-WO_3 nanorods. The cathodic current density at −0.2 V are 17.58, 17.29 and 17.04 mA/cm^2 for m-WO_3 nanoplates; and 23.86, 22.07 and 21.18 mA/cm^2 for m-WO_3 nanorods at 1, 20 and 40 cycles, respectively. The stability for HER of m-WO_3 nanoplates and nanorods were decreased to 1.9 and 5.0% after 40 cycles. In these voltammograms of m-WO_3 nanoplates and nanorods, two kinds of cathodic current density peaks involved during hydrogen evolution were observed at −0.15 V and +0.01 V for m-WO_3 nanoplates, −0.11 V and +0.09 V for m-WO_3 nanorods. These two peaks indicated that hydrogen evolution occurred on different planes of m-WO_3 nanoplates and nanorods. In addition, the different peak potentials and CV behaviors between m-WO_3 nanoplates and nanorods could originate from the different electrocatalysis. In CV results, the former peaks have shown the higher current density than those of the later ones. However, the former was considered as the main plane for hydrogen evolution of m-WO_3 due to their higher cathodic current densities. Thus, for obvious electroactivities of HER, the cathodic current density examined by the

Table 1
Electrocatalytic properties of m-WO_3 commercial, m-WO_3 nanoplates, and m-WO_3 nanorods for HER.

Electrocatalyst	Specific activity at 0.0 V (mA/cm^2)	Specific activity at −0.1 V (mA/cm^2)	Tafel slope[a] (mV/dec)	I_o (mA/cm^2)
m-WO_3 commercial	−0.25	−1.08	−135	0.28
m-WO_3 nanoplates	−1.54	−6.67	−122	1.61
m-WO_3 nanorods	−2.17	−8.61	−113	2.09

[a] In the low over-potential region between +0.010 and −0.015 V.

main plane showed the large cathodic current density of m-WO_3 nanoplates and nanorods with linear sweep voltammograms.

Fig. 7a shows the linear sweep voltammograms of the products at the potential range of −0.100 to +0.075 V. The glassy carbon electrode did not show HER activity under this potential region. The current densities of HER on the m-WO_3 nanoplates and nanorods were more than that of the commercial m-WO_3. The specific activity values of HER at 0.0 and −0.1 V are −0.25 and −1.08 mA/cm^2 for commercial bulk m-WO_3, −1.54 and −6.67 mA/cm^2 for m-WO_3 nanoplates, and −2.17 and −8.61 mA/cm^2 for m-WO_3 nanorods, respectively. Especially for m-WO_3 nanoplates and nanorods, their electroactivities at −0.1 V were 6 and 8 times higher than that of the commercial bulk m-WO_3, respectively. Electrochemical activities of m-WO_3 for hydrogen evolution were enhanced by changing from bulk particles to 2D nanoplates and 1D nanorods.

Tafel plots of commercial m-WO_3, m-WO_3 nanoplates and m-WO_3 nanorods calculated and transferred from their linear sweep voltammograms at low over-potential region between +0.015 and −0.105 V are shown in Fig. 7b. The Tafel slopes for the electrocatalysts (Table 1) of commercial m-WO_3, m-WO_3 nanoplates and m-WO_3 nanorods are −135 mV/dec, −122 mV/dec and −113 mV/dec, respectively. Throughout these Tafel slope, the number of electrons related with hydrogen evolution were also calculated. The number of electrons is 0.88 for commercial bulk m-WO_3, 0.97 for m-WO_3 nanoplates and 1.05 for m-WO_3 nanorods. The 1D m-WO_3 nanorods have shown the highest value among these electrocatalysts, and very close to the theoretical number of electrons for HER. In addition, the exchange current (i_o) density of 1D m-WO_3 nanorods is 2.09 mA/cm^2. This value shows the higher activity than those of the 2D m-WO_3 nanoplates (1.61 mA/cm^2) and commercial m-WO_3 (0.28 mA/cm^2). The higher exchange current density of m-WO_3 nanorods is more appropriate for electrocatalyst than the m-WO_3 nanoplates and commercial m-WO_3, which implied the lower intrinsic resistance for electronic diffusion in the electrochemical reactions [9,28]. These electroactivities are well correlated with the previous unique physical properties such as different morphologies and high crystallinity. Among these products, 1D m-WO_3 nanorods have led to the highest electrochemical activities for hydrogen evolution – originated from the increase in the active sites for electrochemical reactions and rapid electron transfer progressed along with the crystal growth direction in the 1D unique morphology.

Due to these results, m-WO_3 nanoplates and nanorods are believed to preserve the enhanced electrochemical activities and stabilities that are the candidates in electrocatalyst for hydrogen evolution from water.

4. Conclusions

Monoclinic WO_3 nanoplates (2D) and nanorods (1D) were successfully synthesized by the hydrothermal process. The phase of WO_3 was controlled by different kinds of salts and concentrations. Pure phase of m-WO_3 nanoplates was obtained by adding 1.5 g NH_4NO_3 in the solution, and the morphology transformed from m-WO_3 nanoplates to m-WO_3 nanorods by the addition of 1.5 g NH_4NO_3 and 1.0 g PEG to the solution. The electrochemical activities of m-WO_3 nanoplates and nanorods for HER were shown to have the better enhanced activity than the commercial bulk m-WO_3. The unique nanostructured m-WO_3 has shown the new possibility for hydrogen evolution reaction (HER) from water.

Acknowledgements

This work was supported by the Hydrogen Energy R&D Centre, one of the 21st Century Frontier R&D Program and the Brain Korea 21 Program. Dr. Anukorn Phuruangrat is extremely grateful to the Thailand Research Fund (TRF), and the National Research University (NRU) Project for Chiang Mai University, by the Commission on Higher Education (CHE), Ministry of Education, Thailand for financial support for the research at POSTECH, Pohang, Republic of Korea.

References

[1] D. Chen, L. Gao, A. Yasumori, K. Kuroda, Y. Sugahara, Small 4 (2008) 1813–1822.
[2] D. Chen, H. Wang, R. Zhang, L. Gao, Y. Sugahara, A. Yasumori, J. Ceram. Process. Res. 9 (2008) 596–600.
[3] B.I. Kharisov, Recent Pat. Nanotechnol. 2 (2008) 190–200.
[4] X. Shen, G. Wang, D. Wexler, Sens. Actuators B 143 (2009) 325–332.
[5] X. Li, G. Zhang, F. Cheng, B. Guo, J. Chen, J. Electrochem. Soc. 153 (2006) 133–137.
[6] F. Tonus, V. Fuster, G. Urretavizcaya, F.J. Castro, J.L. Bobet, Int. J. Hydrogen Energy 34 (2009) 3404–4309.
[7] S.R. Bathe, P.S. Patil, Smart Mater. Struct. 18 (2009) 025004.
[8] T. Siciliano, A. Tepore, G. Micocci, A. Serra, D. Manno, E. Filippo, Sens. Actuators B 133 (2008) 321–326.
[9] J. Rajeswari, P.S. Kishore, B. Viswanathan, T.K. Vadarajan, Nanoscale Res. Lett. 2 (2007) 496–503.
[10] S.R. Bathe, P.S. Patil, Solid State Ionics 179 (2008) 314–323.
[11] C. Guéry, C. Choquet, F. Dujeancourt, J.M. Tarascon, J.C. Lassègues, J. Solid State Electrochem. 1 (1997) 199–207.
[12] H. Kominami, K. Yabutani, T. Yamamoto, Y. Keraa, B. Ohtan, J. Mater. Chem. 11 (2001) 3222–3227.
[13] A. Wolcott, T.R. Kuykendall, W. Chen, S. Chen, J.Z. Zhang, J. Phys. Chem. B 110 (2006) 25288–25296.
[14] C.N.R. Rao, F.L. Deepak, G. Gundiah, A. Govindaraj, Prog. Solid State Chem. 31 (2003) 5–157.
[15] K. Byrappa, T. Adschiri, Prog. Cryst. Growth Charact. Mater. 52 (2007) 117–166.
[16] F.A. Harraz, Physica E 40 (2008) 3131–3136.
[17] Z. Li, Y. Xiong, Y. Xie, Inorg. Chem. 42 (2003) 8105–8109.
[18] Z. Wang, B. Huang, X. Qin, X. Zhang, P. Wang, J. Wei, J. Zhan, X. Jing, H. Liu, Z. Xu, H. Cheng, X. Wang, Z. Zheng, Mater. Lett. 63 (2009) 130–132.
[19] Q. Han, J. Chen, J. Lu, X. Yang, L. Lu, X. Wang, Mater. Lett. 62 (2008) 2050–2052.
[20] S. Zhong, S. Wang, H. Xu, H. Hou, Z. Wen, P. Li, S. Wang, R. Xu, J. Mater. Sci. 44 (2009) 3687–3693.
[21] J. Ma, Q. Wu, Y. Ding, Nano Part. Res. 10 (2008) 775–786.
[22] Powder Diffract, File, JCPDS Int. Centre Diffract. Data, PA 19073-3273, U.S.A., 2001.
[23] X.C. Song, Y.F. Zheng, E. Yang, Y. Wang, Mater. Lett. 61 (2007) 3904–3908.
[24] Z. Gua, H. Li, T. Zhai, W. Yang, Y. Xia, Y. Ma, J. Yao, J. Solid State Chem. 180 (2007) 98–105.
[25] X. Li, G. Zhang, F. Cheng, B. Guo, J. Chen, J. Electrochem. Soc. 153 (2006) H133–H137.
[26] C. Balázsi, L. Wang, E.O. Zayim, I.M. Szilágyi, K. Sedlacková, J. Pfeifer, A.L. Tóth, P.I. Gouma, J. Eur. Ceram. Soc. 28 (2008) 913–917.
[27] H. Wang, P. Fang, Z. Chen, S. Wang, J. Alloy Compd. 461 (2008) 418–422.
[28] D.J. Ham, R. Ganesan, J.S. Lee, Int. J. Hydrogen Energy 33 (2008) 6865–6872.